

# Development of Bottom-Emitting 1300-nm Vertical-Cavity Surface-Emitting Lasers

D. A. Loudierback, *Member, IEEE*, M. A. Fish, *Member, IEEE*, J. F. Klem, *Senior Member, IEEE*,  
D. K. Serkland, *Member, IEEE*, K. D. Choquette, *Fellow, IEEE*, G. W. Pickrell, *Member, IEEE*,  
R. V. Stone, *Member, IEEE*, and P. S. Guilfoyle, *Senior Member, IEEE*

**Abstract**—We present experimental results on the development of bottom-emitting GaInNAs vertical-cavity surface-emitting lasers (VCSELs) operating at wavelengths near 1300 nm. This development effort is based on the modification of oxide-apertured top-emitting structures to allow emission through the GaAs substrate. Similar device performance was seen in both the top- and bottom-emitting structures. Single-mode output powers (adjusted for substrate absorption) of  $\sim 0.75$  mW, with threshold currents of 1.3 mA, were achieved with  $\sim 3.5$ - $\mu\text{m}$  aperture diameters. Larger multimode devices exhibited a maximum adjusted output power of 2.2 mW. To the best of our knowledge, these are the first bottom-emitting flip-chip compatible 1300-nm VCSELs fabricated with GaInNAs–GaAs active regions.

**Index Terms**—1300 nm, bottom-emitting, flip chip, InGaAsN, optical communications, vertical-cavity surface-emitting laser (VCSEL).

## I. INTRODUCTION

THE DEMAND for inexpensive transmitters for metro-area applications has driven the need for 1300-nm vertical-cavity surface-emitting lasers (VCSELs). The introduction of the GaInNAs material system by Kondow *et al.* [1] has enabled GaAs-based 1300-nm VCSELs with useful operating characteristics to be realized [2]–[4]. The performance of these VCSELs is made possible to a large extent by the availability of oxide current apertures and high-performance AlGaAs–GaAs distributed Bragg reflectors (DBRs). Recent improvements in VCSEL performance, including higher single-mode output powers, lower threshold currents and operating voltages, and lower device resistances, have enabled the use of VCSELs in applications requiring high reliability and operating stability [5].

Although 1300-nm VCSELs can meet the requirements of high-speed interconnects, significant packaging challenges exist with respect to parasitics and impedance matching. The inherently low parasitics of flip-chip bonding can simplify

the packaging, reducing cost and improving performance [6]. Flip-chip bonding is most easily accomplished with devices that have their electrical and optical inputs–outputs on opposite sides of the substrate. Fortunately, band edge absorption in GaAs is negligible at 1300 nm and free carrier absorption is minimal for semi-insulating substrates.

This work demonstrates bottom-emitting flip-chip compatible 1300-nm VCSELs with operating characteristics similar to their top-emitting counterparts. To realize bottom-emitting VCSELs, a typical top-emitting structure was incrementally modified into a bottom-emitting VCSEL. The modified structures allow a meaningful comparison to be made between the top- and bottom-emitting devices. The two modified structures presented in this work, one top-emitting and one bottom-emitting, both utilize a  $1-\lambda$  cavity with three 6-nm GaInNAs quantum wells with 20-nm GaAs barriers. Both structures incorporate a 76.5-nm AlGaAs layer in the first period of the p-mirror for the oxide aperture, as well as a  $5\lambda/4$  n-contact layer within the n-mirror that is not utilized, but imposes the optical loss normally associated with this layer in typical bottom-emitting structures. In addition, the output mirror transmission is nearly the same in both device structures. Both structures were grown by molecular beam epitaxy [7] on n-doped (100) GaAs substrates.

## II. TOP-EMITTING DEVICES

The first device structure used in the development of bottom-emitting GaInNAs VCSELs was a top-emitting structure where a  $5\lambda/4$  n-intracavity contact layer was incorporated into the bottom DBR. Although this intracavity contact layer was not used in the device fabrication, it was included to mimic the optical losses in a typical bottom-emitting structure and make comparisons of device characteristics more straightforward. The top-emitting structure had a linearly graded Si-doped bottom DBR with 35.5 periods and a parabolically graded C-doped top (output) DBR with 20 periods. The doping profiles in both DBRs were designed to minimize resistance and optical loss.

The fabrication procedure for the top-emitting devices started with the deposition of the n-contact metals to the back of the n-GaAs substrate. Next, the p-contact metals were deposited using a ring shape to allow for top emission. The configuration of the p-contact also included a large electrical contact pad to facilitate simple electrical probing. After the emission window was protected with photoresist, chlorine reactive ion etching

Manuscript received June 4, 2003; revised September 16, 2003. This work was supported in part by the Missile Defense Agency (MDA). Sandia National Laboratories is operated by Sandia Corporation, a Lockheed Martin Company, for the U.S. Department of Energy's National Nuclear Security Administration under Contract DE-AC04-94AL85000.

D. A. Loudierback, M. A. Fish, G. W. Pickrell, R. V. Stone, and P. S. Guilfoyle are with OptiComp Corporation, Zephyr Cove, NV 89448 USA (e-mail: duanel@opticomp.com).

J. F. Klem and D. K. Serkland are with Sandia National Laboratories, Albuquerque, NM 87185-0603 USA.

K. D. Choquette is with the Electrical and Computer Engineering Department, University of Illinois at Urbana–Champaign, Urbana, IL 61801 USA.

Digital Object Identifier 10.1109/LPT.2004.824614

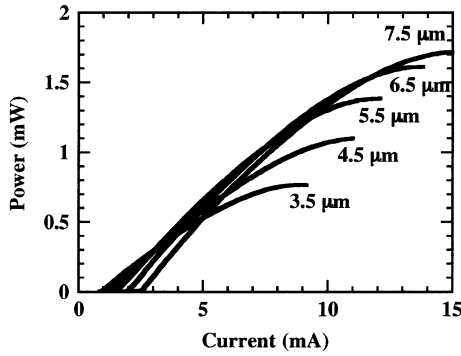


Fig. 1.  $L$ - $I$  characteristics versus aperture diameter for the top-emitting 1300-nm VCSEL structure.

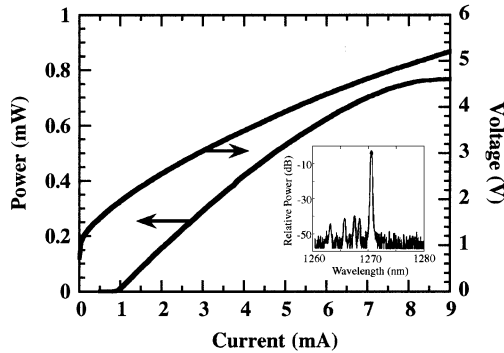


Fig. 2.  $L$ - $I$ - $V$  characteristics for a single-mode top-emitting 1300-nm VCSEL. The inset shows the single-mode lasing spectrum.

(RIE) was used to etch trenches for electrical isolation and aperture oxidation. Finally, the aperture was formed using standard wet lateral oxidation at a temperature of 425 °C. This oxidation process also served to alloy the ohmic metal contacts. Due to the geometry of the p-contact, the area below the probe pad is completely oxidized, ensuring that no parasitic current leakage paths are present. Devices with aperture diameters ranging from below 3–8  $\mu\text{m}$  were fabricated and characterized.

Fig. 1 shows the light-current ( $L$ - $I$ ) characteristics for top-emitting VCSELs with various aperture diameters. Peak output powers of  $\sim 1.75$  mW, with a slope efficiency of 0.2 W/A, were obtained from the larger multimode devices. Size-dependent optical scattering losses from the current aperture forced devices with aperture diameters of less than  $\sim 4$   $\mu\text{m}$  to operate single mode. The threshold current for the single-mode devices was low, with  $\sim 3.5$ - $\mu\text{m}$ -diameter VCSELs having threshold currents of  $\sim 1$  mA. Fig. 2 shows the light-current-voltage ( $L$ - $I$ - $V$ ) characteristics for a typical  $\sim 3.5$ - $\mu\text{m}$ -diameter single-mode VCSEL. The VCSEL had a single-mode output power of  $\sim 0.7$  mW with a threshold current of 0.95 mA and a threshold voltage of 1.93 V. The inset in Fig. 2 shows the lasing spectrum of this single-mode  $\sim 3.5$ - $\mu\text{m}$  VCSEL at a bias current of 5 mA. The peak lasing wavelength is approximately 1267 nm. As can be seen in the figure, this VCSEL had a transverse mode suppression ratio of nearly 40 dB and remained close to this value over the device's operating range.

### III. BOTTOM-EMITTING DEVICES

The bottom-emitting VCSELs had the same basic structure as the top-emitting VCSELs. The only difference was the number of periods in the top and bottom DBRs. For this VCSEL structure, the number of bottom (output) mirror periods was decreased to 24.5, while the number of periods in the top DBR was increased to 35. This modification resulted in a bottom-emitting structure with transmissions for the output and back mirrors that are nearly the same as those of the top-emitting structure. Identical doping levels were also used in these devices to allow a meaningful comparison of the results. As with the top-emitting structure, an n-intracavity contact layer was included in the bottom DBR, but was not utilized for contacting the devices. The devices did have coplanar contacts and pads on the top surface, however, making them flip-chip compatible. The inclusion of the intracavity contact layer does enable future devices to be fabricated on semi-insulating substrates.

The fabrication process for the bottom-emitting devices began with the deposition of circular p-contacts that defined the VCSEL pillars. Using the p-metals as a mask, the structure was etched down to the n-type substrate using chlorine RIE. Next, a ring-shaped n-type contact was deposited on top of the n-type GaAs substrate. This ohmic contact also included a large pad for electrical probing. Finally, using the same conditions as the top-emitting devices, the current aperture was oxidized and the ohmic contacts were alloyed. Again, devices with aperture diameters ranging from below 3 to 8  $\mu\text{m}$  were fabricated and characterized.

Emission through a heavily doped substrate introduces substantial optical loss due to free carrier absorption. To enable a meaningful comparison of top- and bottom-emitting devices, the output powers from the bottom-emitting VCSELs were adjusted to remove the effects of substrate absorption. To estimate the free carrier absorption in the substrate, the following values were used: substrate thickness of 450- $\mu\text{m}$ , n-type doping level of  $\sim 3 \times 10^{18}$   $\text{cm}^{-3}$ , and an n-type free carrier absorption coefficient at 1300 nm of 6  $\text{cm}^{-1}$  (per  $10^{18}$   $\text{cm}^{-3}$  doping) [8]. The output powers of the bottom-emitting VCSELs were estimated by scaling the collected powers by a factor of  $\sim 2.3$ , as derived from the loss described above. While this is only an approximation, the scaling of the data allows a better comparison between the characteristics of the top- and bottom-emitting devices.

Fig. 3 shows the  $L$ - $I$  characteristics for bottom-emitting VCSELs with different aperture diameters. The output powers for these devices were adjusted to remove the effects of free-carrier absorption in the substrate and interface reflections, as previously described. Peak output powers as high as 2.5 mW were obtained from the larger, multimode devices. Large multimode devices exhibited similar slope efficiencies ( $\sim 0.2$  W/A) as the top-emitting VCSELs. In addition, since the top- and bottom-emitting structures have similar size-dependent losses, single-mode operation was again achieved for devices smaller than  $\sim 4$   $\mu\text{m}$ . Fig. 4 shows the  $L$ - $I$ - $V$  characteristics for a typical,  $\sim 3.5$ - $\mu\text{m}$ -diameter single-mode VCSEL. The VCSEL had a single-mode output power of  $\sim 0.75$  mW with a threshold current of 1.15 mA and a threshold voltage of 2.74 V. The

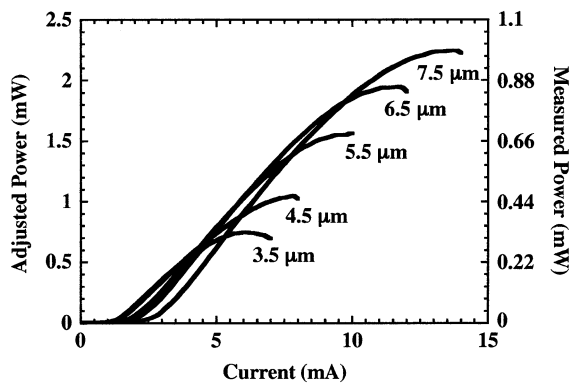


Fig. 3.  $L$ - $I$  characteristics (adjusted for substrate absorption and measured data) versus aperture diameter for the bottom-emitting 1300-nm VCSEL structure.

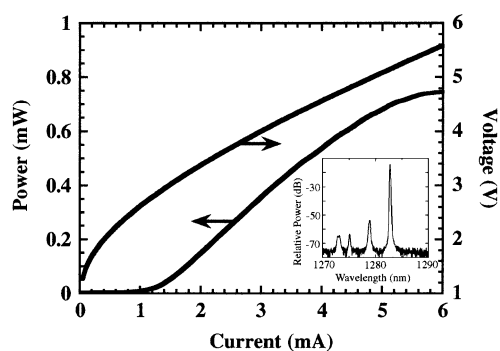


Fig. 4.  $L$ - $I$ - $V$  characteristics (adjusted for substrate absorption) for a single-mode bottom-emitting 1300-nm VCSEL. The inset shows the single-mode lasing spectrum.

operating characteristics of these devices were quite similar to those of the top-emitting devices, although the threshold voltages of the bottom-emitting VCSELS were higher due to poor n-type ohmic contacts. The aperture diameters were estimated, to the nearest  $0.5 \mu\text{m}$ , by finding the smallest pillar size that conducted current. This uncertainty in aperture size leads to the differences in spectral mode spacing seen in Figs. 2 and 4. In addition, the peak output powers of the multimode bottom-emitting VCSELS were significantly higher, possibly due to the lower thermal impedance of the bottom-emitting devices, which had larger pillars. The inset in Fig. 4 shows the lasing spectrum of a single-mode bottom-emitting VCSEL with a peak lasing wavelength of approximately 1283 nm. As the figure shows, this VCSEL had a transverse mode suppression ratio of nearly 40 dB, similar to that of the top-emitting devices.

#### IV. CONCLUSION

By incrementally modifying a typical top-emitting VCSEL structure into a typical bottom-emitting VCSEL structure, top- and bottom-emitting 1300-nm VCSELS with similar designs

have been demonstrated. As expected, the performance of the top- and bottom-emitting 1300-nm VCSELS were similar and showed nearly identical scaling due to size-dependent losses. Both designs exhibited single-mode operation for  $\sim 3.5\text{-}\mu\text{m}$  VCSELS, with threshold currents near 1 mA and peak output powers near 0.75 mW. In addition, output powers (adjusted for substrate absorption) as high as 2.5 mW, were demonstrated for multimode bottom-emitting VCSELS.

The development of bottom-emitting flip-chip compatible 1300-nm VCSELS will enable high-speed operation, particularly in two-dimensional arrays, for future applications. To the best of our knowledge, this work describes the development of the first bottom-emitting GaInNAs VCSELS operating near 1300 nm. In the future, the bottom-emitting device structure will be further modified to incorporate an n-intracavity contact and a semi-insulating substrate to reduce the free-carrier absorption and increase the usable output power. In addition, future efforts will involve flip-chip bonding and high-speed characterization of these devices.

#### ACKNOWLEDGMENT

The authors would like to acknowledge the technical assistance of S. Hawkins, V. M. Montano, and K. M. Geib.

#### REFERENCES

- [1] M. Kondow, K. Uomi, A. Niwa, T. Kitatani, S. Watahiki, and Y. Yazawa, "GaInNAs: A novel material for long-wavelength-range laser diodes with excellent high-temperature performance," *Jpn. J. Appl. Phys.*, vol. 35, pp. 1273–1275, 1996.
- [2] K. D. Choquette, J. F. Klem, A. J. Fischer, O. Blum, A. A. Allerman, I. J. Fritz, S. R. Kurtz, W. G. Breiland, R. Sieg, K. M. Geib, J. W. Scott, and R. L. Naone, "Room temperature continuous wave InGaAsN quantum well vertical-cavity lasers emitting at  $1.3 \mu\text{m}$ ," *Electron. Lett.*, vol. 36, pp. 1388–1390, 2000.
- [3] A. W. Jackson, R. L. Naone, M. J. Dalbearth, J. M. Smith, K. J. Malone, D. W. Kisker, J. F. Klem, K. D. Choquette, D. K. Serkland, and K. M. Geib, "OC-48 capable InGaAsN vertical cavity lasers," *Electron. Lett.*, vol. 37, pp. 355–356, 2001.
- [4] C. S. Murray, F. D. Newman, S. Sun, J. B. Clevenger, D. J. Bossert, C. X. Wang, H. Q. Hou, and R. Stall, "Development of 1.3 micron oxide-confined VCSELS grown by MOCVD," *Proc. SPIE*, vol. 4649, pp. 31–38, 2002.
- [5] L. R. Thompson, L. M. F. Chirovsky, A. W. Jackson, R. L. Naone, D. Galt, S. R. Prakash, S. A. Feld, M. V. Crom, J. G. Wasserbauer, M. D. Lange, B. Mayer, and D. W. Kisker, "Performance of monolithic  $1.3 \mu\text{m}$  VCSELS in telecom applications," *Proc. SPIE*, vol. 4649, pp. 25–30, 2002.
- [6] M. Grabherr, D. Wiedenmann, R. King, R. Jäger, and B. Schneider, "Speed it up to 10 Gb/s and flip chip it: VCSELS today," *Proc. SPIE*, vol. 4649, pp. 11–18, 2002.
- [7] J. F. Klem, D. K. Serkland, and K. M. Geib, "Growth temperature and composition effects in InGaAsN quantum wells for GaAs-based 1300 nm emitters," presented at the Conf. Lasers and Electro-Optics (CLEO), Long Beach, CA, 2002.
- [8] D. I. Babic, J. Piprek, K. Streubel, R. P. Mirin, N. M. Margalit, D. E. Mars, J. E. Bowers, and E. L. Hu, "Design and analysis of double-fused  $1.55\text{-}\mu\text{m}$  vertical-cavity lasers," *IEEE J. Quantum Electron.*, vol. 33, pp. 1369–1383, Aug. 1997.